

Fabrication of microlasers and microresonator optical switches

A. Scherer, J. L. Jewell, Y. H. Lee, J. P. Harbison, and L. T. Florez

Citation: *Appl. Phys. Lett.* **55**, 2724 (1989); doi: 10.1063/1.101935

View online: <http://dx.doi.org/10.1063/1.101935>

View Table of Contents: <http://apl.aip.org/resource/1/APPLAB/v55/i26>

Published by the [American Institute of Physics](#).

Additional information on *Appl. Phys. Lett.*

Journal Homepage: <http://apl.aip.org/>

Journal Information: http://apl.aip.org/about/about_the_journal

Top downloads: http://apl.aip.org/features/most_downloaded

Information for Authors: <http://apl.aip.org/authors>

ADVERTISEMENT



Goodfellow
metals • ceramics • polymers • composites
70,000 products
450 different materials
small quantities fast

www.goodfellowusa.com

Fabrication of microlasers and microresonator optical switches

A. Scherer

Bellcore, Red Bank, New Jersey 07701

J. L. Jewell and Y. H. Lee

AT&T Bell Laboratories, Holmdel, New Jersey 07733

J. P. Harbison and L. T. Florez

Bellcore, Red Bank, New Jersey 07701

(Received 25 July 1989; accepted for publication 17 October 1989)

We have microfabricated low-threshold, high-speed vertical-cavity lasers and optical switches by optimizing the mirror design, crystal growth, and ion etching of microresonators. By minimizing the sidewall ion damage in electrically pumped microlasers, we have defined large arrays of 3- μm -diam surface-emitting devices with threshold currents below 1.5 mA. Ion beam etching was also used to define 0.5–1.5 μm wide all-optical microresonator switches with recovery times as low as 30 ps and controlling energies as low as 0.6 pJ.

With the combination of optimized mirror design and crystal growth, and the use of anisotropic ion etching, we have fabricated micron-sized optical microresonators.¹ These capabilities are now applied to electrically and optically pumped surface-emitting microlasers and other vertical-cavity devices.^{2–6} In order to define the deep structures needed for these applications, highly anisotropic and nonselective ion etching processes must be optimized. Furthermore, masking techniques have to be devised to produce low-resistance contacts for electrically pumped structures. Chemically assisted ion beam etching (CAIBE), a technique in which the sample is simultaneously subjected to both an ion beam and a reactive gas flux, has been demonstrated to be an extremely anisotropic pattern transfer method.⁷ We find that the capabilities of this technique are ideal for solving the problems associated with microfabrication of vertical-cavity optical devices. In this letter we describe the fabrication techniques which we use to produce optically and electrically pumped laser and microresonator arrays.

Alternate layers of AlAs and GaAs were grown on n -type substrates to form $1/4$ wave interference mirrors by molecular beam epitaxy (MBE). These structures were undoped for optically pumped lasers and optical gates, and doped with Be and Si to form p - n junctions for electrically pumped devices. The all-optical devices had a bulk GaAs active region 1.5 μm in thickness between these mirror stacks (Fig. 1). For the surface-emitting lasers, which operate at 983 nm and emit from the back of the wafer, InGaAs quantum wells were used as the active material. These electrically pumped microlasers consisted of 20 $1/2$ half-wave periods of n -doped mirrors on the n^+ substrate, the compositionally graded undoped AlGaAs containing three In_{0.2}Ga_{0.8}As quantum wells, 12 half-wave periods of p -doped mirrors doped to $5 \times 10^{18}/\text{cm}^{-2}$, and a Be delta-doped surface layer which was used to provide a low-resistance top contact to the laser. The electrical contacts were deposited and the delta-doped layer was protected from degradation by thermal evaporation of 150 nm of Au on the surface immediately after removal of the samples from the MBE growth chamber.

Standard photolithography was then performed to deposit masks of either UV stabilized AZ-4110 photoresist or

lift-off masks of nickel or strontium fluoride. Electrical contacts to the n^+ substrate were produced by indium soldering or spark welding a Au-Sn wire to a corner of the laser sample. These prepared samples were then etched in a CAIBE system to transfer the masks into the Fabry-Perot mirror structure. A Kaufman ion source was used to generate ion beams of Ar⁺ and Xe⁺ with a voltage of 1000 eV. The ion flux at the specimen was monitored with a shutter, and maintained at 75 $\mu\text{A}/\text{cm}^2$. The inert gas flow was regulated with a mass flow controller to 4.5 sccm for Xe and 5 sccm for Ar to yield a chamber pressure of $\sim 2 \times 10^{-4}$ Torr. During etching, the sample surface was exposed to a Cl₂ flux of 10 sccm which locally increased the sputter yield. A load-lock sample introduction system was used for fast specimen turnaround, and the base pressure was thereby maintained at below 1×10^{-7} Torr. Under these conditions, the etch rate of Ar⁺/Cl₂ was typically 0.5 $\mu\text{m}/\text{min}$ and the etch rate of Xe⁺/Cl₂ was 1.1 $\mu\text{m}/\text{min}$.

During the pattern transfer in the etching chamber, any instability in the ion current, voltage, or gas pressure results in perturbations of the etched sidewall profile. Since the Kaufman source remains quite stable over short periods of time, very smooth sidewalls can be obtained by etching with

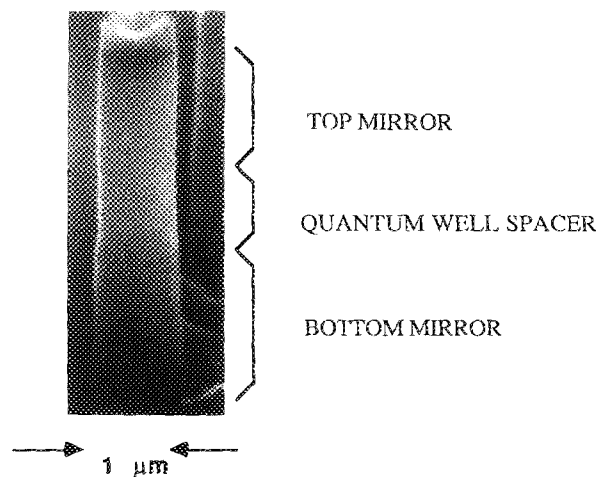


FIG. 1. SEM micrographs of a microresonator etched using AZ-4110 photoresist as a mask.

large etch rates. If the time for which sidewalls are exposed to the reactive gas flux is minimized, chemical attack by the reactive gas can also be decreased. This factor is particularly important when materials with different compositions, such as AlAs and GaAs, are to be etched nonselectively (Fig. 1). The ion etch rate primarily depends on the ion energy, current density, and the partial pressure of the reactive gas at the sample surface. If the substrate is not deliberately heated,

$$\text{etch depth} = (-2.9J^2 + 110f_{\text{Cl}_2}t + 24Jt + 0.67Vt - 1.05 \times 10^{-3}V^2 + 1.2f_{\text{Cl}_2}V + 295J - 8000)/10^4.$$

For any combination of ion energy and flux, the partial pressure of reactive gas (p_{Cl_2}) must be optimized for maximum anisotropy and etch rate. Generally, if p_{Cl_2} is too low, angled sidewalls result and trenches are formed next to the etched microstructures [Fig. 2(a)]. Conversely, when p_{Cl_2} is too high, undercutting of the mask is evident [Fig. 2(b)]. Often, the optimal p_{Cl_2} also depends on the density of the patterns to be etched, since this partial pressure must be increased to compensate for shadowing of the gas jets by closely spaced patterns. To obtain optimal results for widely spaced structures etched with Xe/Cl₂, we use Cl₂ flow rates of 5 sccm, whereas high-density patterns such as are shown in Fig. 3 are optimally etched by using over 10 sccm Cl₂. If the etching process is interrupted, a step results in the sidewall profile. Such a step can be attributed to the oxidation of AlAs mirror layers forming Al₂O₃, which then acts as an ion etch mask.

High etch rates are needed to etch deep features, such as the 5.5 μm microlaser structures, and still retain the necessary vertical sidewall profile. This is particularly important in microresonator mirror structures, where selective etching of AlAs or GaAs can produce very rough sidewalls. In

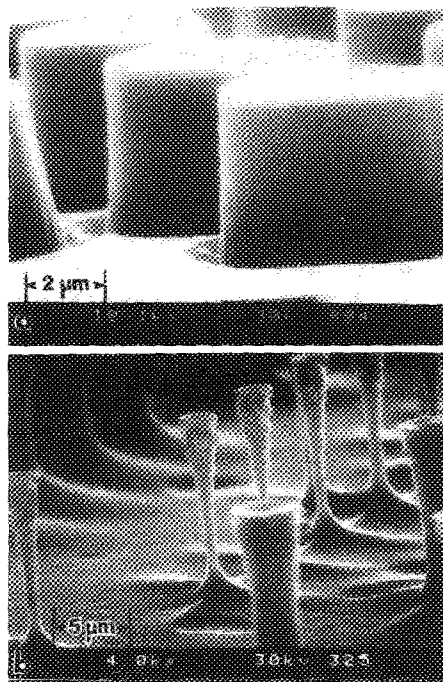


FIG. 2. (a) SEM micrograph of a laser structure defined with Xe⁺/Cl₂ with a low p_{Cl_2} , showing angled sidewalls and trenches around the sidewalls. (b) Undercut laser structures resulting from too large of a p_{Cl_2} at the sample surface during the etch.

the surface temperature can be changed through local heating by altering the ion flux and energy. The interrelationship between etch rate and ion process parameters was derived by performing a simple regression analysis with 24 experiments.⁸ For Ar⁺/Cl₂, in our system geometry, the depth in μm can be approximated by a very complex relationship between ion energy (V) in eV, ion flux (J) in μA/cm², reactive gas flow rate (f_{Cl_2}) in sccm, and time (t) in minutes:

CAIBE, fast and nonselective etching can be obtained by increasing the ion energies above 500 eV. However, at such high ion energies, ion damage can introduce recombination and scattering centers close to the etched vertical sidewalls.^{9,10} To microfabricate low-threshold lasers on the 1–5 μm scale, we therefore not only need to control the sidewall smoothness and the anisotropy of the microfabricated structures, but we also have to minimize the extent of the ion-induced damage to the structure sidewalls. In our CAIBE system, a decrease in the ion energies reduces such damage, but also causes a deterioration of the anisotropy. Instead, we have selected an ion milling species Xe⁺, which with a higher ion mass can produce the required etch rate and anisotropy with reduced ion damage.^{9,11}

The Xe/Cl₂ CAIBE erosion rates of many conventionally used ion etch masks, such as Si₃N₄, SiO₂, or Cr are often too high to use them as masks for the deep structures required for vertical-cavity devices. Instead, good results are obtained by using UV stabilized photoresist,¹⁰ strontium fluoride, or nickel. These materials are stable in a chlorine atmosphere during ion bombardment. SrF₂, a very resistant etch mask which can be deposited by thermal vapor deposition, is optically transparent and thermally stable. This is particularly important if further processing, such as regrowth, is to be performed on the cylinders. A 100-nm-thick SrF₂ mask is sufficient to define 5-μm-deep structures, and produce optically transparent microresonators. Such transparent structures for transmission measurements were produced by chemical removal of the substrate on samples waxed down on glass. After optical lithography and CAIBE of such samples, typical recovery times and controlling energies of 1.5-μm-diam devices were measured as 200 ps and 0.6 pJ, respectively. Similar structures pumped by picosecond optical pulses had lasing thresholds of 9 pJ incident.³ Mi-

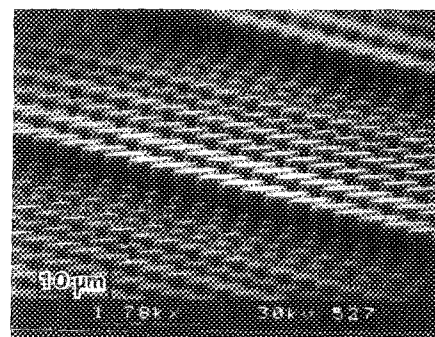


FIG. 3. SEM micrograph of an array of microlasers with dimensions ranging from 1 to 5 μm in diameter. These were etched 5.5 μm deep through the laser structure, and have a 150 nm Au contact on the surface for electrical pumping. The yield of lasing structures above 1.5 μm is close to 100%.

TABLE I. Etch rates of various compounds during CAIBE in Xe^+/Cl_2 at 1000 eV. Etching was done in a Xe^+ ion flux of $75 \mu\text{C}/\text{cm}^2$ and a Cl_2 flow rate of 10 sccm.

GaAs	1000 nm/min
Au	150 nm/min
Ag	75 nm/min
Ni	20 nm/min
SrF_2	20 nm/min
BaF_2	20 nm/min

microresonators as small as $<0.5 \mu\text{m}$ diameter with aspect ratios of 10:1 have been patterned, and these show recovery times of 30 ps at controlling energies of 3 pJ.¹² Other etch resistant masks include vapor-deposited Ni, which is used for the definition of electrically contacted microresonators, such as microlasers. Nickel erodes at only 50% of the rate of chromium and 20% of the rate of gold under the same conditions (Table I). This mask can thus be used to define surface-emitting lasers by first milling through a thick gold contact, and subsequently defining $5.5\text{-}\mu\text{m}$ -deep laser structures without deterioration of the resolution (Fig. 4). A small amount of sidewall roughness is consistently observed near the top of such microlaser structures irrespective of the Ni mask thickness. Since we do not observe this roughness for any uncontacted microresonators, we attribute this effect to the transition between ion milling (of the Au contact) and ion etching (of the GaAs/AlAs mirrors).

MBE growth allows the formation of optical étalons with well-controlled spacings and low loss. In addition, *n*- and *p*-type dopant concentrations can be controllably varied in these mirror structures to provide low-resistance contacts. By defining such material through ion etching into small pillars, large arrays of electrically pumped lasers have been produced (Fig. 3). These surface-emitting microresonators typically exhibit room-temperature, pulsed lasing thresholds of 1.5 mA for $3 \mu\text{m}$ cylinders (Fig. 5). Our smallest microlasers work best when both mirrors have been etched through completely for effective waveguiding, whereas larger structures ($>4 \mu\text{m}$) operate cw at room temperature after etching through only part of the bottom mirror stack to permit more effective heat sinking of the laser cavity. Surface recombination and heating in the small devices presently limit the minimum diameter of measurable microlasers to above $1.5 \mu\text{m}$ and their pulsed thresholds to above 1.0 mA. However, surface passivation¹³ is expected to improve this performance significantly. These structures fail if excessive

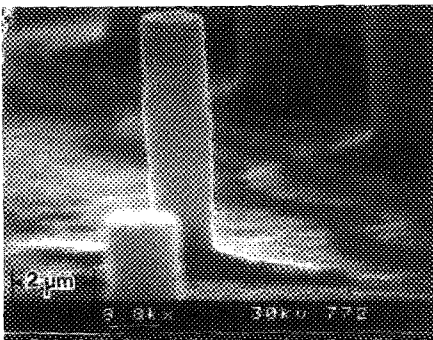


FIG. 4. $1.5\text{-}\mu\text{m}$ -diam microlaser etched under optimum conditions with Xe^+/Cl_2 .

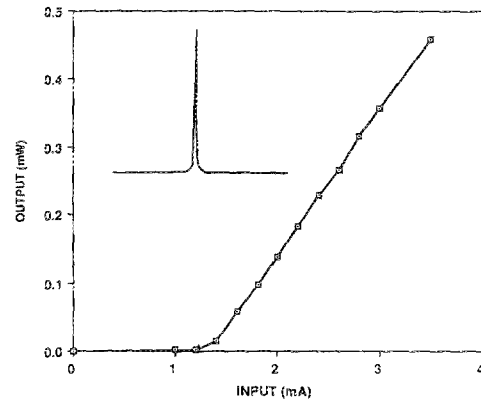


FIG. 5. Pulsed output light vs current behavior of $3\text{-}\mu\text{m}$ -diam electrically pumped surface-emitting laser at room temperature. The differential quantum efficiency is $\sim 16\%$ and the peak full width at half maximum is ~ 0.4 nm.

sidewall damage is introduced during the fabrication, or if the thicknesses of the mirrors and cavity lengths are not calibrated to 1–2%.

Fabrication of micron or submicron-sized vertical-cavity structures allows the integration of a very large number of uniform optical devices ($2 \text{ million}/\text{cm}^2$). The small active volume also allows low-threshold and high-frequency ($>1 \text{ Gb/s}$) operation. However, their definition relies on highly anisotropic etching capabilities using techniques which have only recently been developed for III-V compound semiconductors. We have optimized processes which use such microfabrication to produce extremely small optical components that can be either optically or electrically driven. Surface passivation, the reduction of ion damage, and further optimization of the laser design are expected to significantly improve the performance of these structures in the near future.

The authors wish to acknowledge E. D. Beebe, R. J. Martin, and S. L. McCall for their assistance.

- ¹J. L. Jewell, A. Scherer, S. L. McCall, A. C. Gossard, and J. H. English, *Appl. Phys. Lett.* **51**, 94 (1987).
- ²J. L. Jewell, A. Scherer, S. L. McCall, Y. H. Lee, J. P. Harbison, and L. T. Florez, *Electron. Lett.* Aug (1989).
- ³J. L. Jewell, S. L. McCall, Y. H. Lee, A. Scherer, A. C. Gossard, and J. H. English, *Appl. Phys. Lett.* **54**, 1400 (1989).
- ⁴P. L. Gourley, T. M. Brennan, B. E. Hammons, S. W. Corzine, R. S. Geels, R. H. Yan, J. W. Scott, and L. A. Coldren, *Appl. Phys. Lett.* **54**, 1209 (1989).
- ⁵K. Iga, H. Soda, T. Terakado, and S. Shimizu, *Electron. Lett.* **19**, 457 (1983).
- ⁶L. M. Zinkiewicz, T. J. Roth, L. J. Mawst, D. Tran, and D. Botez, *Appl. Phys. Lett.* **54**, 1959 (1989).
- ⁷G. A. Lincoln, M. W. Geis, S. Pang, and N. Efremow, *J. Vac. Sci. Technol. B* **1**, 1043 (1983).
- ⁸A. Scherer, H. G. Craighead, and E. D. Beebe, *J. Vac. Sci. Technol. B* **5**, 1599 (1987).
- ⁹A. Scherer, H. G. Craighead, M. L. Roukes, and J. P. Harbison, *J. Vac. Sci. Technol. B* **6**, 277 (1988).
- ¹⁰P. Grabbe, A. Scherer, K. Kash, R. Bhat, J. P. Harbison, L. T. Florez, and M. Koza, *Proceedings of the MRS Fall meeting, Boston, Massachusetts, 1988*.
- ¹¹S. Pang, M. W. Geis, N. N. Efremow, and G. A. Lincoln, *J. Vac. Sci. Technol. B* **3**, 398 (1985).
- ¹²J. L. Jewell, S. L. McCall, A. Scherer, H. H. Houh, N. A. Whitaker, A. C. Gossard, and J. H. English, *Appl. Phys. Lett.* **55** (to be published).
- ¹³C. J. Sandroff, M. S. Hedge, L. A. Farrow, C. C. Chang, and J. P. Harbison, *Appl. Phys. Lett.* **54**, 362 (1989).